HHS Public Access

Author manuscript

Sens Actuators B Chem. Author manuscript; available in PMC 2016 December 31.

Published in final edited form as:

Sens Actuators B Chem. 2015 December 31; 221: 379–385. doi:10.1016/j.snb.2015.06.085.

Development of a cobinamide-based end-of-service-life indicator for detection of hydrogen cyanide gas

Lee A. Greenawald[a,*], **Jay L. Snyder**[b], **Nicole L. Fry**[c], **Michael J. Sailor**[c], **Gerry R. Boss**[d], **Harry O. Finklea**[e], and **Suzanne Bell**[e]

[a]Centers for Disease Control and Prevention/National Institute for Occupational Safety and Health/National Personal Protective Technology Laboratory (CDC/NIOSH/NPPTL), 1095 Willowdale Road, Morgantown, WV 26505, USA

[b]113 Snee Drive, Jefferson Hills, PA 15025, USA

[c]Department of Chemistry and Biochemistry, 9500 Gilman Drive, University of California, San Diego, La Jolla, CA 92093, USA

[d]Department of Medicine, 9500 Gilman Drive, University of California, San Diego, La Jolla, CA 92093, USA

[e]C. Eugene Bennett Department of Chemistry, 217 Clark Hall, West Virginia University, Morgantown, WV 26506, USA

Abstract

We describe an inexpensive paper-based sensor for rapid detection of low concentrations (ppm) of hydrogen cyanide gas. A piece of filter paper pre-spotted with a dilute monocyanocobinamide [$CN(H_2O)Cbi$] solution was placed on the end of a bifurcated optical fiber and the reflectance spectrum of the $CN(H_2O)Cbi$ was monitored during exposure to 1.0–10.0 ppm hydrogen cyanide gas. Formation of dicyanocobinamide yielded a peak at 583 nm with a simultaneous decrease in reflectance from 450–500 nm. Spectral changes were monitored as a function of time at several relative humidity values: 25, 50, and 85% relative humidity. With either cellulose or glass fiber papers, spectral changes occurred within 10 s of exposure to 5.0 ppm hydrogen cyanide gas (NIOSH recommended short-term exposure limit). We conclude that this sensor could provide a real-time end-of-service-life alert to a respirator user.

* Corresponding author. ilv1@cdc.gov (L.A. Greenawald)..

Disclaimer

The findings and conclusions in this report are those of the authors and do not necessarily represent the views of the National Institute for Occupational Safety and Health. Mention of product name does not constitute endorsement by the National Institute for Occupational Safety and Health or the Centers for Disease Control and Prevention.

Author contributions

The manuscript was written through contributions of all authors. All authors have given approval to the final version of the manuscript.

Appendix A. Supplementary data

Supplementary data associated with this article can be found, in the online version, at http://dx.doi.org/10.1016/j.snb.2015.06.085

Keywords

Paper sensor; Optical sensor; Hydrogen cyanide; Cobinamide; Diffuse reflectance; End-of-service-life indicator

1. Introduction

The National Institute for Occupational Safety and Health (NIOSH) defines a level of 50 ppm as immediately dangerous to life or health (IDLH) for hydrogen cyanide gas (HCN) [1]. HCN is present in manufacturing industries such as electroplating, mining, production of paper, textiles, plastics and pesticides. It is considered a potential chemical warfare agent, having been used in both World Wars I and II, and in recent terrorist attacks [2–4].

In occupational or military settings, persons who may be exposed to HCN are required to wear a self-contained breathing apparatus (SCBA) or an air-purifying respirator (APR) fitted with a NIOSH-approved chemical, biological, radiological, nuclear (CBRN) canister. It is often difficult for users to determine when the activated carbon bed becomes saturated and reaches its “end-of-service-life” (ESL). The smell or irritation of a gas has been used to indicate breakthrough but by the time a user can smell a gas, dangerous concentrations may already be present. According to OSHA 1910.134, sensory warning properties cannot be used to determine cartridge/canister change-out [5]. Software models provided by manufacturers are currently used to help users estimate when breakthrough will occur [5]. Unfortunately, unpredictable input data such as types and concentrations of toxic chemicals, relative humidity, and breathing rate may not be readily available to the user. In addition, most of the theoretical models incorporated into the software are for organic vapors.

In 1984, NIOSH published standards for certification of sensors indicating breakthrough (termed “end-of-service-life indicators” or ESLIs,) to encourage their development [6]. The sensors are intended to provide a real-time alert to indicate to the user that the canister is near its maximum absorption capacity and vapor breakthrough is imminent. ESLI standards require a reliable sensor to indicate sorbent depletion at 90% canister volume [7]. Current challenges in developing these sensors for incorporation into respirators include the effects of humidity, as well as size, weight, and power restrictions. Additionally, manufacturers prefer to limit costs to no more than $1 per canister for the sensor and $20–$50 for the sensor-related fixturing and electronics per respirator [6]. Only a few colorimetric and qualitative ESLIs are available (such as for mercury vapor), and these rely on subjective visual detection to identify a color change [8,9]. These are inappropriate in poorly lit environments or for color blind persons.

One possible ESL sensor design is based on optical measurement of a colored compound dispersed on a white medium. The availability of small photodetectors, inexpensive optical fibers, and low-power LED light sources suggest that a simple diffuse reflectance configuration could satisfy the size, cost, and power requirements. In addition, paper is inexpensive and easily obtainable. Common sample media for diffuse reflectance include soil [10], paint [11], body tissues [12], crystals [13] and paper [14,15]. To obtain a linear

relationship of spectral intensity to sample concentration, the Kubelka–Munk equation may be applied:

$$F(R) = \frac{(1-R)^2}{2R} = K/S \quad (1)$$

where R is reflectance, K is the absorption coefficient, and S is the scattering coefficient. The Kubelka–Munk formula is the most common approach to interpret diffuse reflectance and make the data comparable to that of transmittance [16].

Paper is a promising substrate for real-time, low-cost sensors. It is lightweight, adaptable to varied size and shape requirements, compatible with chemicals of various matrices, and has high wicking ability [17]. Paper is also highly porous with a large surface area, which is advantageous for rapid adsorption of gas-phase analytes. A known potential disadvantage of using paper is irreproducibility that can occur when using detection systems close to the paper's surface; this can be attributed to inhomogeneous coating of the indicator and the resulting diffusion. Nery and Kubota provide an extensive review on current "lab-on-paper" techniques [18]. The ubiquity of paper makes it a suitable support medium to incorporate into an economical and portable sensor.

With paper selected as the substrate, a compatible indicating system must be selected. Cobinamide (Cbi), a cobalt-centered hydroxocobalamin analog, can bind up to two cyanide (CN^-) ions. The structure is shown in Fig. 1, where the X and Y ligands can be OH^-, H_2O, or CN^-. A cyanide ion rapidly displaces a water or hydroxyl ligand on cobinamide, with an overall K_a value of $10^{22}M^{-2}$ (compared to a K_a value of $10^{12}M^{-1}$ for hydroxocobalamin), shown below [19].

$$OH(H_2O)Cbi \xrightarrow{10^{14}M^{-1}} CN(H_2O) \xrightarrow{10^{8}M^{-1}} (CN)_2Cbi$$

At neutral pH in water, Cbi exists as the mixed hydroxyaquo complex $OH(H_2O)$Cbi, termed aquohydroxocobinamide [20]. As noted by Baldwin et al. [21] and further shown by Ma et al. [20], more rapid and pronounced spectral changes occur on CN^- binding when starting with monocyanocobinamide [$CN(H_2O)$Cbi] than when starting with either diaquacobinamide or aquohydroxocobinamide; this is attributed to the stronger trans-labilizing effect of CN^- compared to OH^-. The change from $CN(H_2O)$Cbi to dicyanocobinamide [$(CN)_2$Cbi] yields a significant color change from orange (peak absorbance at ~510 nm) to violet (583 nm) that is easily observed. Complexing of $CN(H_2O)$Cbi with CN^- can be detected at concentrations as low as 0.25 nM cyanide in solution [20,22]. Using a 583 nm LED, a cobinamide-saturated qualitative filter paper and a photodiode detector, 13.5 ppb HCN released from 1 mL of acidified blood has been detected [23]. In addition to vitamin B12 derivatives, triphenylamine-based chemodosimeters have reported naked-eye detection as low as 1.8 ppm [24]. Chemical ionization mass spectrometry (CIMS) and selected ion flow tube mass spectrometry (SIFT-MS) have reported LODs of 5 ppt and 8 ppt HCN, respectively [25,26]. Portable electrochemical detectors are widely available and detect HCN in the occupational range of interest of

0.0-100.0 ppm with LOD of 0.5 ppm [27]. Although commonly used, these portable detectors are too large to be useful as an ESLI. The latest developments of CN^- and HCN detection can be found in a review by Randviir [28].

NIOSH designates maximum exposure limits for many occupational hazard gases. A short-term exposure limit (STEL) is a 15 min time-weighted average that should not be exceeded at any time during a 10 h work day [29]. HCN has a STEL of 4.7 ppm [29]. For the proposed HCN-specific ESLI, a response to 5.0 ppm HCN must occur within minutes. Here we harness the distinct and rapid color change exhibited by cobinamide binding to CN^- from HCN gas to generate a paper-based diffuse reflectance device.

2. Experimental

2.1. Chemicals and materials

Aquohydroxocobinamide [$OH(H_2O)$Cbi], Co(III) was synthesized from hydroxocobalamin as described previously [30]. Potassium cyanide (KCN) was purchased from Fisher Scientific (granular; certified ACS) and was dissolved in 1 M NaOH (Fisher Scientific, certified). Stock HCN gas was purchased from Butler Gas (Pittsburgh) at a concentration of 495.0 (±2%) ppm. Fisherbrand® P8 Qualitative filter paper (200 μm thick, 20-25 μm particle retention) and Gelman Sciences A/E Borosilicate Glass fiber filter paper (without binder, 330 μm thick, 1 μm pore size) were used as the support media. Deionized water was from an 18 MΩ cm deionized in-line water system (Thermo Scientific Micropure).

2.2. Preparation of cobinamide solution

A bench-top ultraviolet–visible (UV–VIS) spectrometer (Thermo Scientific Evolution 300) was used to determine the concentration of cobinamide stock solutions using a molar extinction coefficient of $2.8 \times 10^4 M^{-1}\ cm^{-1}$ [31]. The concentration of dicyanocobinamide [(CN_2)Cbi] was determined using a molar extinction coefficient at 583 nm of 10,450 $M^{-1}\ cm^{-1}$. Binding of one cyanide ion to $OH(H_2O)$Cbi was achieved by incubating equimolar amounts of cobinamide and KCN overnight at 4 °C. $CN(H_2O)$Cbi stock solutions were diluted in deionized water to 50.0 ± 0.2 μM for fixing onto the paper substrates.

2.3. Preparation of paper substrates

Filter paper was cut into uniform 6.0 ± 0.5 mm diameter circles. A volume of 15.00 ± 0.02 μL 50 μM Cbi was placed onto the center of each piece of paper leading to approximately 0.9 μg $CN(H_2O)$Cbi per paper. The $CN(H_2O)$Cbi solution diffused uniformly on the paper substrate and was allowed to dry fully at room temperature (~21 °C). Some samples were tested at 50 and 85% relative humidity (%RH) by incubating the Cbi-spotted paper at the respective %RH for 4 h at 21.0 °C using an environmental chamber (Caron Model 6010-1) prior to the beginning of the experiment.

The average apparent absorbance of $CN(H_2O)$Cbi on cellulose filter paper (measured at 500 nm) was 0.14 ± 0.02 a.u. (F(R) value equal to 0.049 ± 0.001) with a 16%CV. The average apparent absorbance on glass fiber filter paper was 0.18 ± 0.03 a.u. (F(R) value equal to

0.089 ± 0.002) with 14%CV for glass fiber paper. These values are based on 30 samples for both cellulose and glass fiber filter paper with ± values of ±1 s.

2.4. Diffuse reflectance instrumentation

An Ocean Optics USB4000 UV-VIS-ES miniature spectrometer (200-850 nm) was used for diffuse reflectance measurements. The Cbi-impregnated paper circles were inserted into a custom-made holder constructed of black, Delrin® plastic. A 12.7 mm diameter mirror (Thor Labs BB05-E02) was incorporated into a screw-top lid at top of the holder, above the paper circle. Two holes in each side of the holder allowed HCN to pass through the holder; the holder is shown in Fig. S1 (Supplementary Material). The common end of a bifurcated fiber optic (Ocean Optics, core diameter 600 μm, fused silica) was connected to the bottom of the holder directly under the filter paper. The two distal branches of the fiber were connected to a tungsten halogen light source (Ocean Optics LLS, 215-2500 nm) and the USB spectrometer, respectively.

2.5. HCN flow experimental setup

The experimental setup is shown in Fig. S2. Three mass flow controllers (MFCs; Alicat Scientific) regulate air flow, the HCN concentration, and the percent relative humidity (%RH). The %RH was measured with a humidity sensor prior to each experiment and the HCN concentration was confirmed using an HCN-specific electrochemical detector (Interscan RM, 0-50.0 ± 0.1 ppm) [32]. Experiments were performed at a carrier gas flow rate of 1 liter per minute (LPM) at 25%RH (unless otherwise specified) at room temperature. HCN gas from the cylinder was diluted with air to the desired HCN concentration (1.0-10.0 ppm), and the final concentration was verified using the Interscan HCN detector. The lowest concentration at which an accurate dilution could be obtained was 1.0 ppm. All tubing was made of Teflon (PFTE) material.

The system was initially flushed with air at the desired %RH (no HCN) for 1-2 h before the experiment. The system was evaluated by the Interscan to ensure a reading of 0.0 ppm HCN. A blank paper circle was then placed in the holder. The reflectance signal from the blank was defined as 100% reflectance at each wavelength. A piece of CN(H_2O)Cbi-impregnated paper was then placed in the holder and the appropriate reflectance spectrum recorded. In some experiments, the reflectance spectrum of CN(H_2O)Cbi-doped paper was designated as the blank when the goal was to monitor changes in the CN(H_2O)Cbi spectrum. The paper circles were allowed to equilibrate with the desired %RH for 30 min in the holder prior to beginning the experiment. Initially, a three-way valve was set to allow air to flow to the Interscan HCN detector. Once the Interscan sensor read the desired HCN concentration, the valve was switched to direct the air to flow over the sensor. The valve switching time was designated as the start of the experiment.

3. Results and discussion

3.1. System optimization

3.1.1. Instrument—For the cellulose filter paper, the integration time of the spectrometer was set at 600 ms, with a boxcar width and scans-to-average set to give. The integration

time for an individual scan was selected to give a signal 85% of the spectrometer's saturation level (limited by the A/D converter to 65k counts), while the number of scans-to-average was chosen to optimize signal-to-noise. The glass fiber filter paper used was thicker than the cellulose paper and allowed more light to be reflected back to the detector. Thus, the integration time was set to 300 ms with a boxcar width and scans-to-average set to five. The spectrometer software measures the intensity of reflected light returning back to the detector from the paper through the bifurcated fiber optic and converts the data to an apparent absorbance.

Absorbance was converted to reflectance (Eq. (2)) and then to the Kubelka–Munk Function (Eq. (1)) by:

$$R=10^{-A} \quad (2)$$

where A is absorbance (a.u.).

3.1.2. Flow—The flow rate over the paper was set to 1 LPM to avoid back pressure build-up in the sensor holder. This flow rate has no correlation to the air flow through a canister but was chosen to focus on studying the binding between HCN and $CN(H_2O)$Cbi. The small size of the sensor box combined with the 1 LPM flow rate yields a time constant of a few seconds for a step change in HCN concentration.

3.1.3. Volume and concentration of cobinamide—The optimal concentration of $CN(H_2O)$Cbi to pipette onto the paper substrate was found to be 50.0 ± 0.2 μM. This concentration yielded a reflectance spectrum with a high signal to noise ratio without being too concentrated, which would result in lower sensitivity in detecting small changes of the reflectance spectrum.

The optimal volume of $CN(H_2O)$Cbi placed onto the paper circles was 15.00 μL ± 0.02, which completely wicked over the surface of the paper without oversaturating and leaving $CN(H_2O)$Cbi residue outside the paper. This volume allowed the paper substrates to dry within 1 h.

3.2. UV–VIS spectra of cobinamide

The absorbance spectra for $OH(H_2O)$Cbi, $CN(H_2O)$Cbi, and $(CN)_2$Cbi in aqueous solution at 20 μM are shown in Fig. 2. The absorbance spectra for $OH(H_2O)$Cbi and $CN(H_2O)$Cbi are similar, thus the changes in absorbance spectrum when trace amounts of CN^- bind to $OH(H_2O)$Cbi are not analytically useful. When a second cyanide ion binds to $CN(H_2O)$Cbi, a peak appears at 583 nm, absorption at 450-500 nm decreases, and an isosbestic point occurs at 531 nm.

The absorption spectrum of a 50 μM $CN(H_2O)$Cbi solution is similar to the diffuse reflectance spectra of $CN(H_2O)$Cbi on cellulose and glass fiber papers (Fig. 3A). The spectra of Cbi both in aqueous solution and on paper are similar. A higher *K/S* value (Eq. (1)) for $CN(H_2O)$Cbi is observed on the glass fiber paper than on the cellulose filter paper,

likely due to the greater thickness of the glass fiber paper reflecting more light to the detector.

3.3. Cbi detection of HCN

3.3.1. Cellulose filter paper—The average blank signal on cellulose paper measured in the range 570-590 nm in terms of the Kubelka–Munk function is 6 (± 1) × 10^{-7}, or in terms of absorbance: 0.0005 ± 0.0002 a.u. (n = 10). Statistically, the limit of detection (LOD) using cellulose filter paper in terms of the Kubelka–Munk function is 3.1 × 10^{-6}, or 0.001 a.u. using LOD = $3\sigma + \bar{x}$

Fig. 3B shows the spectral changes that result from the conversion of $CN(H_2O)$Cbi to $(CN)_2$Cbi when excess KCN (in 1 mM NaOH) is added to a $CN(H_2O)$Cbi solution in a cuvette (absorbance spectrum) and when 15.0 ppm HCN flows over a Cbi-impregnated glass fiber paper for 15 min (diffuse reflectance). There is a slight variation between the absorbance spectrum and diffuse reflectance spectrum, but the characteristic features of the dicyano complex are apparent by diffuse reflectance. Thus, substitution of the water ligand by cyanide occurs readily for the $CN(H_2O)$Cbi on the paper.

Fig. S3a (Supplemental Information) shows the response of $CN(H_2O)$Cbi on cellulose filter paper when exposed to 5.0 ppm HCN after 1 and 5 min at 25%RH. The Kubelka–Munk function is plotted for the diffuse reflectance spectra. The increased signal at 583 nm, decreased signal at 450-500 nm and isosbestic point at 531 nm are apparent. This is more easily seen in Fig. S3b where the spectrum of $CN(H_2O)$Cbi on filter paper was the blank, creating difference spectra. The characteristic spectral shifts are similar to those reported in Ma et al. and Blackledge et al. for CN^- binding to $OH(H_2O)$Cbi [20,22].

Two $F(R)$ vs. time trends, one at 583 nm and the other at the average response of 450-500 nm, are shown in Fig. S4a. T = 0 corresponds to the time at which the valve was turned to direct the HCN gas over the sensor. As expected, exposure to 5.0 ppm HCN shows a higher signal at 583 nm (and lower signal at 450-500 nm) than exposure to 1.0 ppm HCN. Fig. S4b displays an expansion of Fig. S4a as the initial response when HCN passes over the sensor. With an estimated dead time of less than 2 s for the start of the cyanide flow, a measurable response at 583 nm appears within 10 s for a 5.0 ppm exposure. A slower response is observed for a 1.0 ppm exposure, with an increase in signal occurring at approximately 20 s.

3.3.2. Glass fiber filter paper—The average blank signal on glass fiber filter paper measured in the range 570-590 nm in terms of the Kubelka–Munk function is 8 (± 1) × 10^{-9}, or in terms of absorbance: 0.00005 ± 0.00009 a.u. (n = 10). The LOD (LOD = $3\sigma + \bar{x}$) using glass fiber filter paper in terms of the Kubelka–Munk function is 2.8 × 10^{-7}, or 0.0003 a.u. These values are lower than those obtained for cellulose filter paper.

Using the glass fiber paper and plotting the Kubelka–Munk function for the diffuse reflectance spectra, a similar pattern is observed: the 583 nm signal increases and the 450-500 nm signal decreases when 5.0 ppm HCN is present at 25%RH (Fig. 4A). Unlike the signal from cellulose paper, the signal from the glass fiber paper levels off at longer HCN exposure times, with a near steady-state signal observed within 10 min of exposure. This

observation is likely attributed to the larger surface area of the thicker glass fiber paper and more cobinamide available to complex with CN^-. This is also more easily visualized in Fig. 4B where the spectrum of $CN(H_2O)$Cbi on glass fiber filter paper is the blank, creating difference spectra. Similar to the cellulose paper, Fig. 5A shows $F(R)$ vs. time at 583 nm for 5.0 ppm and 1.0 ppm, where a larger signal is observed for the 5.0 ppm HCN exposure. Fig. 5B shows a rapid initial response occurring within 5 s for 5.0 ppm HCN exposure, while the initial rapid rise occurs over ~10 s for the 1.0 ppm exposure. Compared to cellulose filter paper, the glass fiber paper displays initial response times approximately half those of the cellulose paper.

A comparison between the response of cellulose filter paper and glass fiber filter paper when exposed to 5.0 ppm HCN for 15 min is shown in Fig. S5. The response with the glass fiber filter paper is significantly larger than with the cellulose filter paper. Although 5.0 ppm of HCN is the primary concentration of interest, the glass fiber paper displays increased Kubelka–Munk values ($F(R)$) at every HCN concentration for each time interval when compared to cellulose filter paper. For 5.0 ppm HCN, the Kubelka–Munk function is linear for cellulose paper but nonlinear for glass fiber paper with respect to time (Fig. S6). The saturation of the response suggests that the amount of reacted cobinamide complex is approaching the total amount of cobinamide immobilized in the paper. The linear behavior for cellulose paper indicates that the amount of reacted cobinamide is small with respect to the total amount of cobinamide over the 15 min of exposure. These differences indicate that the interaction of $CN(H_2O)$Cbi with the substrate affects its response to HCN.

The Kubelka–Munk signal is linear with respect to HCN concentration after 1 min (Fig. S7a) as well as after 15 min (Fig. S7b) with R^2 values 0.9885 and 0.9943, respectively. Deviations are most likely due to the nonhomogeneous medium. One of the assumptions of the Kubelka–Munk function is that the substrate is isotropic and homogenous, which is not the case here [33]. An improved linear correlation using the Kubelka–Munk function is observed after 15 min exposure, most likely due to the system being at steady state at each concentration. Although the Cbi-impregnated filter papers can detect HCN concentrations of less than 5.0 ppm, the focus of this study is the STEL of HCN and we found that HCN at 5.0 ppm can be detected in less than 1 min using the $CN(H_2O)$Cbi-impregnated paper.

3.4. Effect of percent relative humidity (%RH) on HCN detection

The effect of %RH on the paper's detection performance was quantified for RH values of 50 and 85%. These humidity values (including 25%RH) were evaluated because respirators are used in a wide range of climates with various temperatures and humidity. Fig. 6A shows the response on cellulose filter paper as a function of time for varying %RH, with data and expansion of the initial response in the Supplementary Material (Table S5, Fig. S8a, and Table S6). A data point was added to Fig. 6A indicating the average F(R) at 583 nm for 25% RH after 60 min (0.030 ± 0.001), similar to the $F(R)$ values of 50 and 85% RH after only 15 min (0.035 ± 0.001 and 0.0358 ± 0.0001, respectively). At each %RH, the signal responds at approximately the same time (~10 s) after exposure to HCN. The faster response of the $CN(H_2O)$Cbi-impregnated paper for high relative humidity is clearly evident in this figure. Fig. 6B shows data for the glass fiber, with data and expansion of the initial response in the

Supplementary Material (Table S5, Fig. S8b, and Table S7). These $F(R)$ values are much higher than those observed for the cellulose filter paper. The response for 25%RH starts to plateau after 10 min, while the response for 50 and 85%RH starts to plateau after 5 min for 50% and close to 1 min for 85%RH, reaching steady state much more rapidly than cellulose paper. The cellulose and glass fiber filter papers both show a larger signal and a faster response at the wavelengths of interest at higher %RH. This observation may be attributed to the ability of the papers to absorb water vapor [34]. The adsorbed water may create a more solution-like medium for the reaction between HCN and cobinamide. It is also possible a higher response is due to a smaller scattering cross-section for both types of paper as water fills the air-filled pores of the paper [34].

The large value of the binding constant for cyanide with $CN(H_2O)Cbi$ (10^8) implies that the cyanide binding should be irreversible. However, Fig. 7 shows that the complex can slowly revert back to $CN(H_2O)Cbi$ when HCN is removed from the gas stream. HCN was cycled on and off at 15 min increments with an additional 60 min absence of HCN at the end of the experiment. Surprisingly, the rate of loss of cyanide was greatest at 50%RH compared to 25% and 85%RH. The rate of loss of cyanide appears to be slower than the rate of binding. In terms of an ESLI, a brief exposure to HCN may not trigger the sensor due to insufficient change in the reflectance spectrum. However, the sensor would remain sensitive and respond rapidly upon a repeated exposure to HCN (i.e. if the user moved in and out of contaminated air). However, the initial detection at a specific point within the canister (e.g. representing 10% service-life remaining) from the wavefront HCN would indicate to the user that the canister must be immediately replaced, as per ESLI standards and user instructions [7,35]. Alternatively, the onset removal of environmental HCN, regardless of %RH, would unlikely cause full reversibility; the CN^- within the activated carbon would redistribute and eventually reach the sensor location again by diffusion [36].

4. Conclusions

We demonstrated an inexpensive paper-based optochemical sensor for detecting low concentrations (1.0-10.0 ppm) of HCN gas. The sensor has potential to be used as an end-of-service-life indicator in respirators. Cobinamide-impregnated filter papers can detect the NIOSH-recommended STEL concentration for HCN gas within 10 s of HCN exposure. A more rapid response occurs under conditions of higher humidity, and the Kubelka–Munk function yields a more linear signal as a function of HCN exposure time and concentration.

This work shows proof of concept that an ESLI could be developed to indicate to the user that the canister service-life has almost ended. The sensor would work as follows: the sensor would be embedded with direct contact to the carbon bed of a canister. Once HCN reaches a fixed point prior to breakthrough, the sensor would rapidly respond due to a change in the cobinamide spectrum. When a defined threshold is reached, an alarm would indicate to the user that the canister must be quickly replaced.

The availability of small photodetectors, inexpensive optical fibers, and battery-powered LED light sources suggest that the simple diffuse reflectance configuration could be modified to satisfy the size, cost, and power requirements of ESLIs. The small footprint of

the device makes it feasible to incorporate other sensing elements (for VOCs, halogens, CWAs, etc.) in a multiplexed fashion. The cobinamide sensing element has the potential to detect other compounds known to complex with cobinamide, such as ammonia and hydrogen sulfide [37].

Supplementary Material

Refer to Web version on PubMed Central for supplementary material.

Acknowledgements

The authors acknowledge financial support from CDC/NIOSH/NPPTL for the funding of this project.

Biographies

Lee A. Greenawald is a Ph.D. candidate in the C. Eugene Bennett Department of Chemistry at West Virginia University and physical scientist student trainee at CDC/NIOSH in Morgantown, WV. She received her B.S. degree in Forensic Chemistry from Ohio University in 2011. Her research interests include the development of inexpensive and portable sensors that have potential to be used with a respirator to protect users against breathing toxic gases. She has presented at various analytical and forensic-related conferences.

Jay L. Snyder received a B.S. in Chemical Engineering from West Virginia University and a M.S. in Occupational Health from the University of Pittsburgh's Graduate School of Public Health. He has worked in the occupational health field for the past forty years where he gained extensive background in health issues associated with mining. In 2001, he took a position with the National Institute for Occupational Safety and Health (NIOSH) at the National Personal Protective Technology Laboratory (NPPTL). There he developed the End of Service Life (ESL) program for personal protective equipment.

Nicole L. Fry received her Ph.D. from UC Santa Cruz in the area of inorganic chemistry. She is currently a post-doctorate fellow working with Gerry Boss and Michael Sailor at UC San Diego. Her project has focused on loading cobinamide into porous silicon for sensing and drug delivery applications.

Michael J. Sailor is Professor and Leslie Orgel Scholar in Inorganic Chemistry in the department of Chemistry and Biochemistry and at the University of California, San Diego. He is also an Affiliate Professor in the Departments of Bioengineering, Nanoengineering, and in the Materials Science and Engineering Program at UCSD.

Gerry R. Boss is Professor of Medicine at the University of California, San Diego. A major area of his research interest is in developing countermeasures to toxic chemicals. He found that cobinamide is not only an effective cyanide countermeasure, but also that it could be used to quantitatively measure low amounts of cyanide.

Harry O. Finklea is a professor in the C. Eugene Bennett Department of Chemistry at West Virginia University. His research interests include electrochemistry, fuel cells (especially solid oxide fuel cells), self-assembled monolayers on electrodes, and sensors.

Suzanne Bell is an associate professor in the C. Eugene Bennett Department of Chemistry and in the Forensic and Investigative Sciences Department at West Virginia University. Her research interests are in applied and forensic analytical chemistry, chemometrics, and forensic toxicology.

References

[1]. CDC. Hydrogen cyanide. NIOSH Pocket Guide to Chemical Hazards. Apr. 2011 Retrieved from http://www.cdc.gov/niosh/npg/npgd0333.html (accessed 10.01.15)

[2]. CDC. Hydrogen cyanide (AC): systemic agent. NIOSH Education and Information Division. The Emergency Response Safety and Health Database. May. 2011 Retrieved from http://www.cdc.gov/niosh/ershdb/emergencyresponsecard 29750038.html (accessed 10.01.15)

[3]. Stewart, C. Cyanide as a Chemical Weapon: A Review. Retrieved from http://www.firesmoke.org/wp-content/uploads/2010/10/Cyanide As_A_Weapon.pdf (accessed 11.01.15)

[4]. HHS. Chemical warfare. U.S. National Library of Medicine. Aug. 2014 Retrieved from http://sis.nlm.nih.gov/enviro/chemicalwarfare.html (accessed 12.01.15)

[5]. CDC. Respirator trusted-source information. The National Personal Protective Technology Laboratory (NPPTL). Aug. 2011 Retrieved from http://www.cdc.gov/niosh/npptl/topics/respirators/disp part/RespSource3end.html (accessed 11.01.15)

[6]. Rose-Phersson S, Williams ML. Integration of Sensor Technologies in Respirator Vapor Cartridges as End-of-Service Life Indicators: Literature and Manufacturers Review and Research Roadmap. 2005

[7]. NIOSH. Determination of End of Service Life Indicator (ESLI) Test, Air-Purifying Respirators Standard Testing Procedure (STP). NPPTL Laboratory; Pittsburgh, PA.: 2005. p. 6

[8]. Safety, Honeywell. N Series Catridges and Filters. Retrieved from http://honeywellsafety.com/ (accessed 3.01.15)

[9]. North, Cartridge and Filter Reference Chart. Retrieved from http://www.unitedfireandsafety.com/Userfiles/Docs/Cartridge Filter Chart.pdf (accessed 23.02.15).

[10]. Samuels AC, Zhu C, Williams BR, Ben-David A, Miles RW, Hulet M. Improving the linearity of infrared diffuse reflection spectroscopy data for quantitative analysis: an application in quantifying organophosphorous contamination in soil. J. Anal. Chem. 2006; 78:408–415.

[11]. Monico L, Janssens K, Miliani C, Van der Snickt G, Brunetti BG, Guidi MC, Radepont M, Cotte M. Degradation process of lead chromate in paintings by Vincent van Gogh studied by means of spectromicroscopic methods. artificial aging of model samples of co-precipitates of lead chromate and lead sulfate. J. Anal. Chem. 2013; 85:860–867.

[12]. Yu B, Sha A, Nagarajan VK, Ferris GG. Diffuse reflectance spectroscopy of epithelial tissue with a smart fiber-optic probe. Biomed. Opt. Express. 2014; 5:675–689. [PubMed: 24688805]

[13]. Lee SJ, Han SW, Choi HJ, Kim K. Phase behavior of organic-inorganic crystal: temperature-dependent diffuse reflectance infrared spectroscopy of silver sterate. Eur. Phys. J. D. 2001; 16:293–296.

[14]. Luiz VHM, Pezza L, Pezza HR. Determination of nitrite in meat products and water using dapsone with combined spot test/diffuse reflectance on filter paper. Food Chem. 2012; 134:2546–2551. [PubMed: 23442723]

[15]. Momin SA, Narayanaswamy R. Optosensing of chlorine gas using a dry reagent strip and diffuse reflectance spectrophotometry. Anal. Chim. Acta. 1991; 244:71–79.

[16]. Myrick ML, Simcock MN, Baranowski M, Brooke H, Morgan SL, McCutcheon JN. The Kubelka–Munk diffuse reflectance formula revisited. Appl. Spectrosc. Rev. 2014; 46:140–165.

[17]. Liana DD, Raguse B, Gooding JJ, Chow E. Recent advances in paper-based sensors. Sensors. 2012; 12:11505–11526. [PubMed: 23112667]

[18]. Nery EW, Kubota LT. Sensing approaches on paper-based devices: a review. Anal. Bioanal. Chem. 2013; 405:7573–7595. [PubMed: 23604524]

[19]. Brenner M, Mahon SB, Lee J, Kim J, Mukai D, Goodman S, Kreuter KA, Ahdout R, et al. Comparison of cobinamide to hyroxocobalamin in reversing cyanide physiologic effects in rabbits using diffuse optical spectroscopy monitoring. J. Biomed. Opt. 2010; 15:017001-1–017001-8. [PubMed: 20210475]

[20]. Ma J, Dasgupta PK, Zelder FH, Boss GR. Cobinamide chemistries for photometric cyanide determination: a merging zone liquid core wavequide cyanide analyzer using cyanoaquacobinamide. Anal. Chim. Acta. 2012; 736:78–84. [PubMed: 22769008]

[21]. Baldwin DA, Betterton EA, Pratt JM. The chemistry of vitamin B12. Part 20. Diaquocobinamide: pK values and evidence for conformatinal isomers. J. Chem. Soc.: Dalton Trans. 1983:217–223.

[22]. Blackledge WC, Blackledge CW, Griesel A, Mahon SB, Brenner M, Pilz RB, Boss GR. New facile method to measure cyanide in blood. J. Anal. Chem. 2010; 82:4216–4221.

[23]. Ma J, Ohira S, Mishra SK, Puanngam M, Dasgupta PK, Mahon SB, Brenner M, Blackledge W, Boss GR. Rapid point of care analyzer for the measurement of cyanide in blood. Anal. Chem. 2011; 83:4319–4324. [PubMed: 21553921]

[24]. Gotor R, Costero AM, Gil S, Parra M, Martínez-Máñez R, Sancenón F, Gaviña P. Selective and sensitive chromogenic detection of cyanide and HCN in solution and in gas phase. Chem. Commun. 2013; 49:5669–5671.

[25]. Le Breton M, Bacak A, Muller JBA, O'Shea SJ, Xiao P, Ashfold MNR, Cooke MC, et al. Airborne hydrogen cyanide measurements using a chemical ionization mass spectrometer for the plume identification of biomass burning forest fires. Atmos. Chem. Phys. 2013; 13:9217–9232.

[26]. Španel P, Dryahina K, Smith D. The concentration distributions of some metabolites in the exhaled breath of young adults. J. Breath Res. 2007; 1:1–8.

[27]. MSA. ALTAIR Pro Single-Gas Detector. Retrieved from http://us.msasafety.com/Portable-Gas-Detection/Single-or-Two-Gas/ALTAIR%26reg%3B-Single-Gas-Detector/p/000080000200001010 (accessed 10.06.15)

[28]. Randviir EP, Banks CE. The latest developments in quantifying cyanide and hydrogen cyanide. Trends Anal. Chem. 2015; 64:75–85.

[29]. CDC. Hydrogen cyanide. Pocket Guide to Chemical Hazards. 2011. Retrieved from http://www.cdc.gov/niosh/npg/npgd0333.html (accessed 15.01.15)

[30]. Broderick KE, Gingh V, Zhuang S, Kambo A, Chen JC, Sharma VS, Pilz RB, Boss GR. Nitric oxide scavenging by the cobalamin precursor cobinamide. J. Biol. Chem. 2005; 280:8678–8686. [PubMed: 15632180]

[31]. Ford SH, Nichols A, Shambee M. The preparation and characterization of the diaquo-forms of several incomplete corrinoids cobyric acid, cobinamide, and three isomeric cibinic acid pentaamines. J. Inorg. Biochem. 1991; 41:235–244. [PubMed: 2056308]

[32]. Interscan, Rack-Mount Analyzers – Hydrogen Cyanide. Retrieved from http://catalog.gasdetection.com/viewitems/search-by-gas-type-hydrogen-cyanide/rack-mount-analyzers-rm-series-hydrogen-cyanide (accessed 15.01.15)

[33]. Džimbeg-Malčić V, Barbarić-Mikočević Ž, Itrić K. Kubelka–Munk theory in describing optical properties of paper (I). Tech. Gaz. 2011; 1:117–224.

[34]. Ellerbee AK, Phillips ST, Siegel AC, Mirica KA, Martinez AW, Striehl P, Jain N, Pretniss M, Whitesides GM. Quantifying colorimetric assays in paper-based microfluidic devices by measuring the transmission of light through paper. Anal. Chem. 2009; 81:8447–8452. [PubMed: 19722495]

[35]. 3M, 3M Mercury Vapor/Chlorine Gas Cartridge/Filter 60629, P100 Respiratory Protection, St. Paul, MN, 2015, Retrieved from http://solutions.3m.com/wps/portal/3M/en_US/GovernmentSolutions/Home/ProductInformation/ProductCatalog/~/3M-Mercury-Vapor-Chlorine-Gas-Cartridge-Filter-60929-P100-Respiratory-Protection-60-EA-Case?N=5928575+4294933553&rt=d (accessed 01.06.15)

[36]. EPA. Section 6.0: Carbon Adsorbers. p. 36Retrieved from http://www.epa.state.oh.us/portals/27/engineer/eguides/carbon.pdf (accessed 10.06.15)

[37]. Salnikov DS, Makarov SV, van Eldik R, Kucherenko PN, Boss GR. Kinetics and mechanism of the reaction of hydrogen sulfide with diaquacobinamide in aqueous solution. Eur. J. Inorg. Chem. 2014:4123–4133. [PubMed: 25580081]

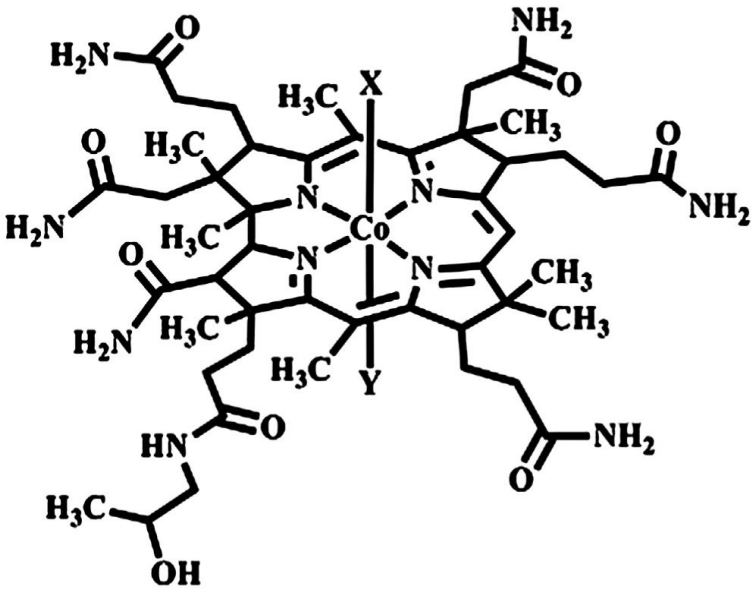

Fig. 1.
Structure of cobinamide (Cbi).

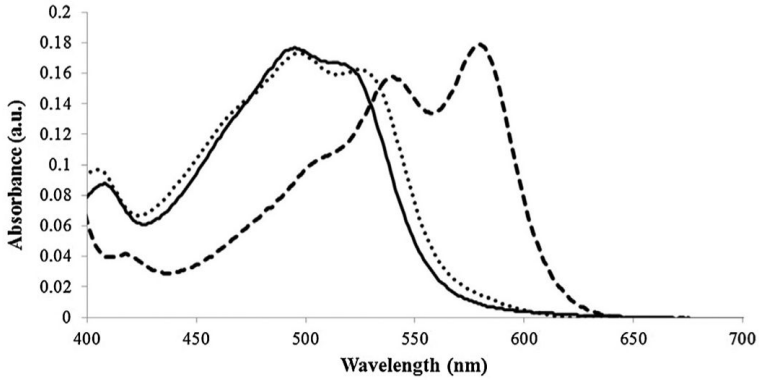

Fig. 2.

Spectra of the three cobinamide complexes: $OH(H_2O)$Cbi (solid line), $CN(H_2O)$Cbi (dotted line) and (CN_2)Cbi (dashed line).

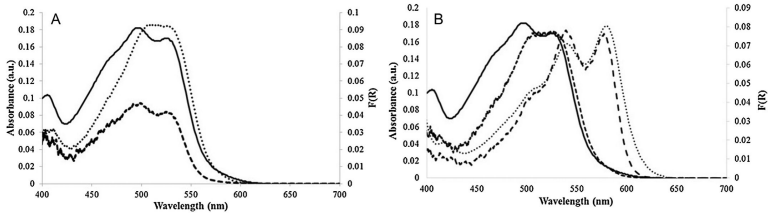

Fig. 3.

(A) Comparison of monocyanocobinamide solution spectra and diffuse reflectance spectra on cellulose and glass fiber filter paper. The Kubelka–Munk function is plotted for the diffuse reflectance spectra. Solution spectra for 20 μM $CN(H_2O)Cbi$ (solid line); diffuse reflectance on cellulose filter paper (dashed line) and diffuse reflectance spectra on glass fiber filter paper (dotted line). (B) Comparison of monocyanocobinamide solution spectra and diffuse reflectance spectra on glass fiber paper. Solution spectra for 20 μM $CN(H_2O)Cbi$ in solution before excess KCN is added (solid line) and after KCN is added (dotted line). Diffuse reflectance spectra for $CN(H_2O)Cbi$ on glass fiber paper before excess HCN gas is introduced (short dashed line) and after HCN exposure (long dashed line).

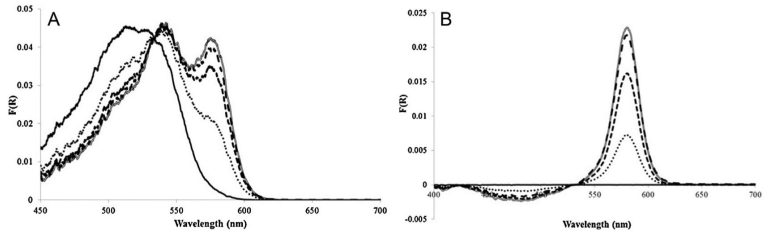

Fig. 4.

(A) Monocyanocobinamide response to 5.0 ppm HCN exposure on glass fiber filter paper as a function of time of exposure. CN(H_2O)Cbi before HCN (solid line), 1 min of exposure (dotted line), 5 min of exposure (short dashed line), 10 min exposure (long dashed line) and 15 min exposure (hollow line). (B) Diffuse reflectance spectra when the reflectance spectrum of CN(H_2O)Cbi on glass fiber filter paper was designated as the “blank” (solid line), 1 min exposure (dotted line), 5 min exposure (short dashed line), 10 min exposure (long dashed line) and 15 min exposure (hollow line).

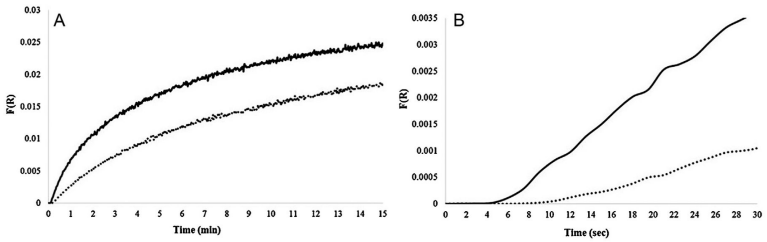

Fig. 5.

(A) $CN(H_2O)Cbi$ on glass fiber paper response to 1.0 and 5.0 ppm HCN. 5.0 ppm HCN response at 583 nm (black line), 1.0 ppm HCN response at 583 nm (dotted line). (B) Expanded version of the initial response (in s) to 5.0 ppm HCN at 583 nm (solid line) and 1.0 ppm HCN at 583 nm (dotted line).

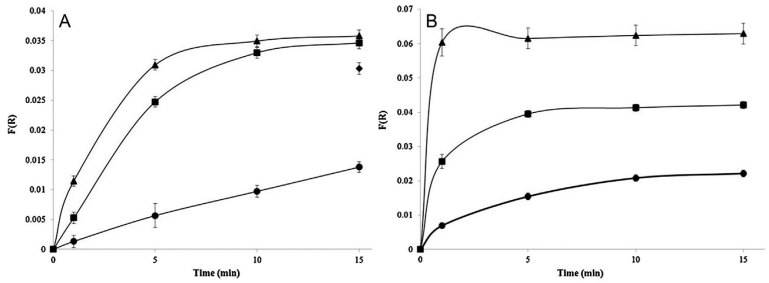

Fig. 6.

(A) Average response of CN(H_2O)Cbi on cellulose filter paper to 5 ppm HCN gas as a function of time of exposure at 25%RH (circle), 50%RH (square) and 85%RH (triangle). Error bars are represented by 95% C.I. for $n = 3$. (B) Average response of CN(H_2O)Cbi on glass fiber filter paper to 5.0 ppm HCN at various exposure times at 25%RH (circle), 50%RH (square) and 85%RH (triangle). Error bars are represented by 95% C.I. using $n = 3$ for 50%RH and 85%RH and $n = 6$ for 25%RH.

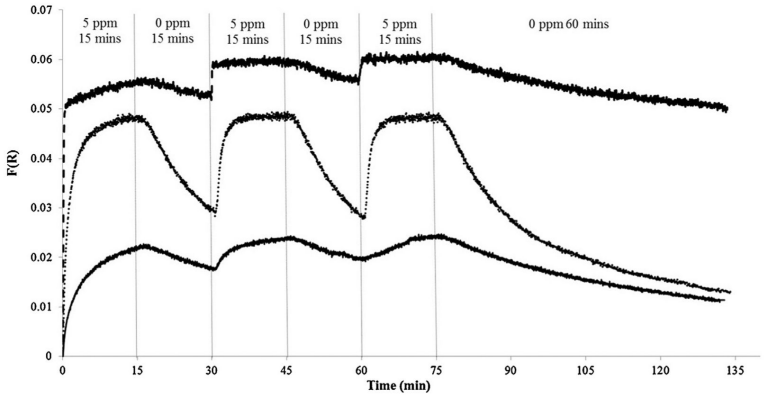

Fig. 7.

Cycling of 5.0 ppm HCN exposure at various %RH. 25%RH at 583 nm (solid line), 50%RH at 583 nm (dotted line), 85%RH at 583 nm (dashed line).